Chapter 3

Imaging Evaluation of Liver Tumors in Pediatric Patients

Chengzhan Zhu, Bingzi Dong and Qian Dong

Additional information is available at the end of the chapter

http://dx.doi.org/10.5772/intechopen.73855

Abstract

Imaging plays crucial roles in the management of pediatric patients with suspected liver malignant tumors. Three-dimensional (3D) imaging could significantly improve the resection rate of pediatric tumors and increase the safety of the surgery. With the development of medical imaging, 3D reconstruction technology, the innovation of liver surgery and the proposal of precise hepatectomy, the intrahepatic vascular anatomy of the liver and liver segmentectomy based on that vascular anatomy have become well developed. With the analysis of 3D digital liver, we proposed a new type of liver classification system: Dong's digital liver classification system. And we measured the normal total liver volume from neonate to aging making a reference for surgeons all around the world. And the Human Digital Liver Database was established by the Affiliated Hospital of Qingdao University and Hisense Company, aiming to collect digital liver from neonates, children, adults, and the elderly, from normal livers, livers with cancer, and simulated livers resected using Hisense CAS. Then we showed one case report of patient with giant liver tumor. With the application of Hisense CAS and our data, we successfully removed the tumor. We believe that the new techniques in imaging will help surgeons to accomplish better operations.

Keywords: three-dimensional imaging, liver tumor, digital liver classification, total liver volume, Human Digital Liver Database

1. Introduction

Liver tumors constitute 1–4% of all solid tumors in children, of which 40% are benign. They mainly include hemangioma, liver hamartoma, and liver cell adenoma. Malignant tumors mainly include hepatoblastoma (HB), hepatocellular carcinoma (HCC), malignant liver

mesothelioma, and rhabdomyosarcoma [1]. For most hepatic malignancies, hepatectomy or liver transplantation is optimal for cure. Resectability can be limited by multifocality, bilobar involvement, vascular thrombus or vascular invasion, extension to hepatic hilum, and distant metastasis [2]. If the tumor cannot be resected at initial imaging evaluation, the child is usually first treated with chemotherapy and/or radiation, and then re-imaged. For this reason, proper imaging evaluation of the liver is necessary which will shorten the surgical waiting duration and increase the success of the resection. In the cases where liver resection has high morbidity and high incidence, liver transplantation is recommended.

Imaging plays crucial roles in the management of pediatric patients with suspected liver tumors. MR imaging is recommended for children than computed tomography (CT) because of less radiation [3, 4]. However, CT could clearly show the liver anatomy and be helpful in staging, which is widely used in preoperative evaluation in the pediatric patients [3, 5]. Moreover, if the CT or MR imaging indicates a malignant mass, CT of the chest should be performed to assess the presence of lung metastasis [6].

In our experience, three-dimensional imaging can significantly improve the resection rate of pediatric tumors and increase the safety of the surgery [7]. In our center, we prefer CT scans for preoperative evaluation of pediatric liver tumors. However, it is very important to avoid non-contrast and multiphase images, and use low-dose CT scan in pediatric patients. CT phase of portal venous are very useful for evaluation of primary malignant liver tumors in children.

2. Common malignant liver tumors in pediatric patients

2.1. Hepatoblastoma (HB)

HB comprises 1% of all pediatric malignancies. HB most often occurs in infants and young children between 6 months and 4 years old. The median age of occurrence is 18 months. After 5 years of age, it becomes rare but histologically more aggressive in children over 8 years old. It occurs equally in males and females [8]. Based on radiological imaging, preoperative staging system (Pretreatment Extent of Disease or PRETEXT) which define extent of liver parenchyma involvement is an important guideline for treatment selection [9]. The new international surgical guidelines, which are being developed for the upcoming Pediatric Hepatic International Tumor Trial, will recommend primary surgical resection at diagnosis for PRETEXT I and II tumors of which the radiographic margin on the middle hepatic vein is wide [10].

As staging and treatment are mainly dependent on imaging, high-quality radiographic imaging has come to be of vital importance. For imaging assessment, both contrast-enhanced CT and MRI are recommended. Non-contrast CT typically shows a relatively well-defined, heterogeneous mass, slightly hypodense compared with liver tissue, with or without calcifications. On contrast-enhanced CT (**Figure 1**), the tumor reveals a heterogeneous enhancement, which may be hyperdense relative to liver parenchyma in the early arterial postcontrast phase and usually appears iso- or hypodense on delayed images (11). Invasion of the portal vein and its subsequent thrombosis must be evaluated in all suspected cases of hepatoblastoma. The tumor thrombus can even spread along IVC and encroach in the lumen of right atrium.

http://dx.doi.org/10.5772/intechopen.73855

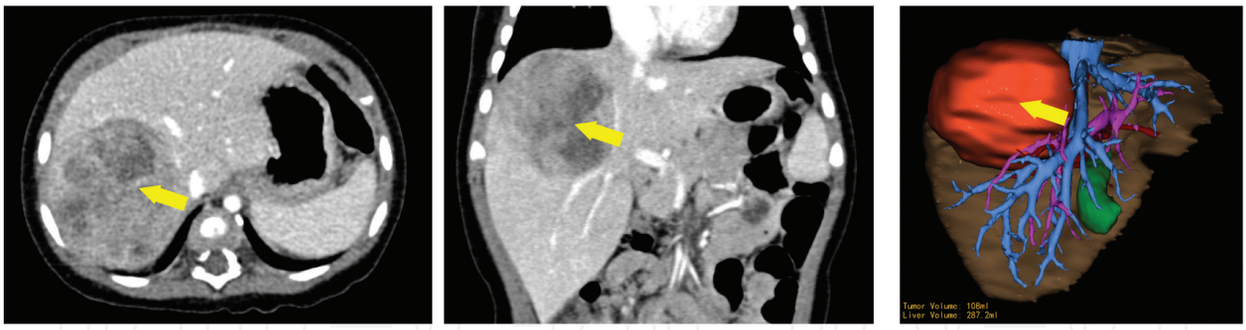

Figure 1. CT and three-dimensional reconstructed liver of PRETEXT II hepatoblastoma resectable at diagnosis (white arrow).

Metastasis may be seen in lymph nodes and lung parenchyma; it is rare in the brain and bones [11]. Twenty percent of HBs present with metastasis and most of them are in the lungs; therefore CT chest is necessary for staging.

2.2. Hepatocellular carcinoma (HCC)

The incidence of HCC in children was 0.5–1.0 cases per million children [12]. Different from HB, the median age of occurrence in children with HCC is 10 to 11.2 years [3]. The male to female ratio is 2:1 in young children, but it increases with age. Unlike adults, in whom HCC usually accompanies underlying liver disease, only 20–35% of children with HCC children have underlying liver disease [13]. HCC in children is now considered a distinct tumor family consisting of adult type HCC and variants, fibrolamellar HCC, and transitional liver cell tumor [14]. HCC is usually multifocal and may present with a variable number and distribution of tumor nodules. Recognizing HCC lesions smaller than 1.0 cm is still difficult.

In fibrolamellar HCCs, tumor cells are circumscribed by bundles of acellular collagen. This form is seen more frequently in adolescents than in adults and has better prognosis. HCCs are highly variable and show non-characteristic features on CT imaging: the tumors may be homogeneous or heterogeneous, solitary or multifocal, well- or ill-defined. On unenhanced CT images, HCCs typically appear isodense or slightly hypodense relative to liver parenchyma. On enhanced CT, they show early arterial contrast enhancement and rapid washout. HCCs are often inconspicuous on delayed scans. HCC sometimes invades the vasculature in the liver, and even the inferior vena cava may be seen [11]. The diagnosis of underlying cirrhosis may help during differential diagnosis, but it is rare in children. Three-dimensional CT image (**Figure 2**) analysis techniques are now available to estimate tumor volume and provide detailed information regarding the intrahepatic anatomy that resembles the actual intraoperative findings [15]. CT volumetry may permit calculation of resected tumor volume and anticipated size of the remnant liver in planning resection [16]. Plain CT of the chest should be performed to rule out the lung metastases. As for HB, tumor staging is an important consideration in determining the plan of treatment and prognosis. The PRETEXT staging system is recommended because it is currently the only staging system that allows surgical planning [9]. HCC is relatively chemoresistant. Complete resection or liver transplantation of localized tumor is the best option. In the SIOPEL-1 report, the overall resection rate was 36% and the 5 y OS and EFS was 28 and 17% respectively [13]. For liver transplantation, patient survival was

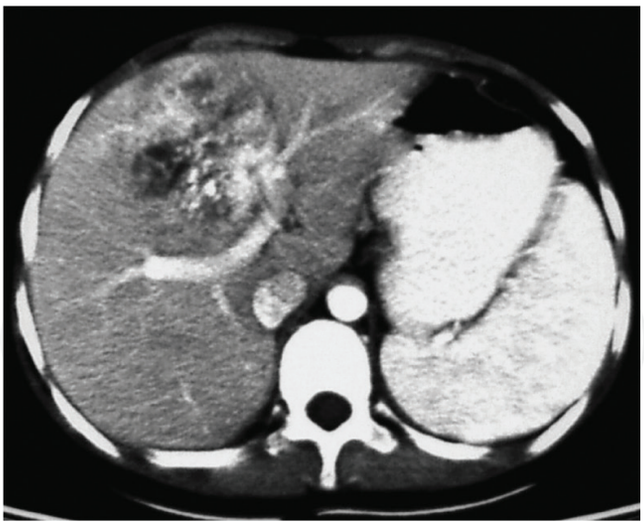

Figure 2. CT of hepatocellular carcinoma in pediatric patient.

63% at 5 years and 58% at 10 years in a study of orthotopic liver transplantation in 41 HCC children <18 years. Recurrence was the primary cause of death in 86% [17]. The outcomes of liver transplantation in HCC are not as good as that for HB.

2.3. Pediatric hepatic sarcomas

Pediatric hepatic sarcomas include undifferentiated embryonal sarcoma (UES), biliary rhabdomyosarcoma, and angiosarcoma [5]. UES is a rare malignant neoplasm, and its the incidence is higher than the other two types of sarcoma. UES was recently shown to share genetic features with mesenchymal harmatoma. Diagnosis of UES is usually between 6 and 10 years but some studies report presentation in young teenagers [18]. The tumor appears on ultrasound as a hetero-echoic mass, and a hypodense multicystic lesion on CT scan or MRI (**Figure 3**), usually exceeding 10 cm in size, with a predominance for involving the right hepatic lobe [19].

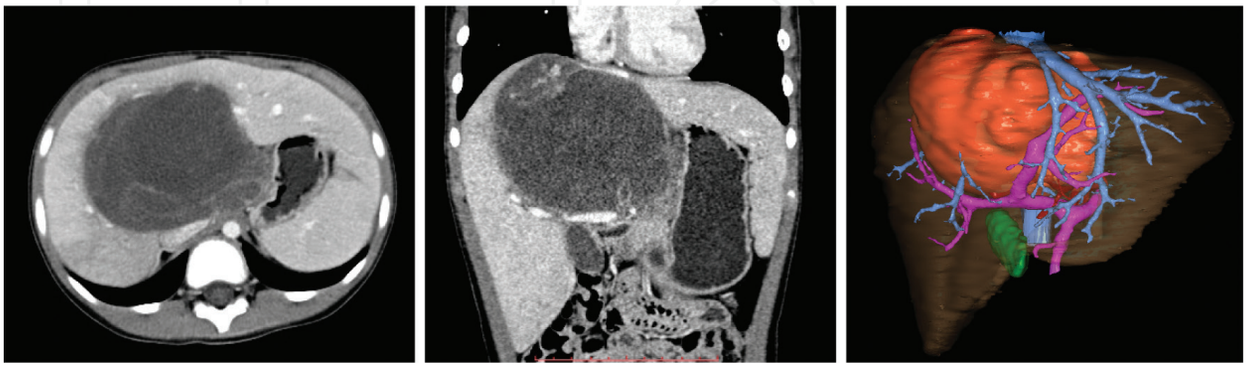

Figure 3. CT and three-dimensional reconstructed liver of undifferentiated embryonal sarcoma.

http://dx.doi.org/10.5772/intechopen.73855

3. Value of CT scan in guiding the surgical treatment

The objective of surgery is to achieve complete resection of the tumor, both macro- and microscopically, which is paramount for cure of malignant liver cancers. The liver resection strategy is based on pre-operative understanding of liver segmentation, vascular occlusion techniques, and experience in performing different types of hepatectomy, including extensive resection (left and right trisegmentectomies). Although abdominal CT should only be considered if MR imaging is not available or contraindicated, there are some limitations of MRI in some hospitals at developing countries. In our experience, MRI is the best available technique for diagnosing liver tumors, but its value is less clear in preoperatively evaluating the resectability of liver tumors especially in pediatric patients. The development and rapid clinical acceptance of single-detector helical CT during the last decade and, more recently, the introduction of multidetector CT (MDCT) have resulted in significant improvements in the study of the liver. MDCT makes it possible to precisely image the vascular anatomy, including the anomalous branches, feeding arteries, or drainage veins. Moreover, each image phase could be independently and simultaneously extracted or combined. In addition to technical advances, such as shorter scanning times, multiplanar imaging, and improved ability to perform multiphasic contrast-enhanced studies, newer and better intravenous contrast media and advances in post-acquisition data processing techniques have renewed researchers' enthusiasm for using hepatic CT scanning [11].

Furthermore, the software program for volumetry provides a proposed remnant liver volume and an optimal cut line of the liver. Various preoperative simulations can thus be considered. This volumetric analysis positively contributes to the safety of the procedure by assisting in the selection of the optimal operations. Preoperative evaluation of the relationship between the tumor and surrounding vasculature was simulated to perform liver resection with 3D software (**Figure 4**).

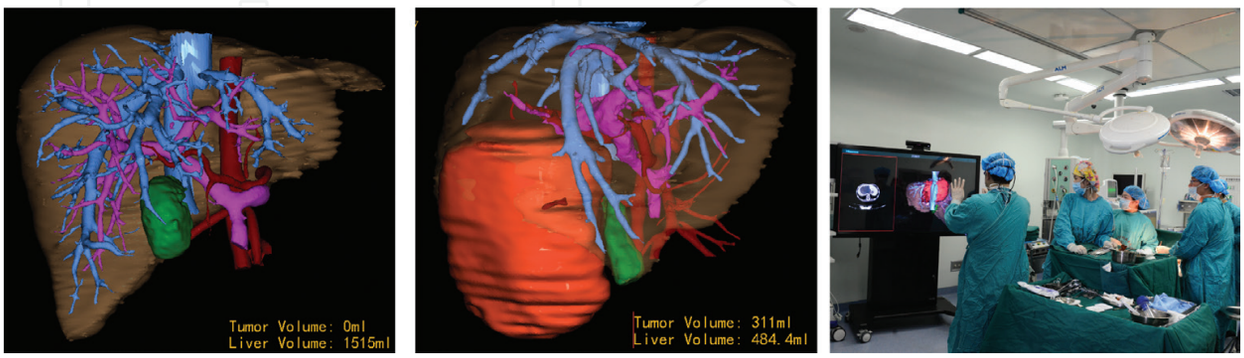

Figure 4. Three-dimensional reconstructed liver indicating total liver volume, liver tumor volume, and intraoperative navigation system.

4. 3D simulation software and Hisense Computer Assisted Surgery System (Hisense CAS)

With the development of three-dimensional simulation software, it is possible to achieve virtual hepatectomy, which can assist the surgeons planning the operation. The development of three-dimensional simulation software makes it possible to achieve virtual hepatectomy, which can assist surgeons to plan the operation, especially the complicated one. The history of 3D simulation software as it relates to hepatectomy can be divided into three stages: [1] successful 3D rendering of liver structures due to the introduction of multidetector row CT in the 1990s [20, 2] virtual hepatectomy depending on the reconstruction of the liver using 3D simulation software since 2000 [21, 3] the clinical practice and popularization of virtual hepatectomy using software packages since 2005, such as operation planning and operative navigation [22]. In some developed countries, such as Japan, virtual hepatectomy has routinely been performed in adult patients undergoing anatomic liver resection. It helps surgeons to plan the operative approach precisely, accurately position the lesion range, and be familiar with the operative route. Hisense Computer Assisted Surgery System (Hisense CAS) is a 3D simulation software package specifically developed for pediatric patients. It can provide precise and exquisite 3D visualization of pediatric liver structures using DICOM data from conventional CT. Considering that children have more refined anatomical structures, the accuracy of Hisense CAS was improved. Hepatectomy can be simulated on a personal computer, and the results can be shared with anyone in the cooperative team. Hisense CAS allows a surgeon to instantaneously manipulate the liver simulation in the operating room using a gesture-controlled display (**Figure 4**).

CT imaging can be performed using a 64-row-MDCT Scanner (Sensation64; Siemens, Erlangen, Germany) with the following parameters: kVp 120, mAs 100, slice collimation 0.625 mm, feed/rotation 12 mm, and rotation time 0.5 s. Patients received 2.0 ml/kg of an iodinated contrast agent (Ultravist; Bayer HealthCare LLC, Germany) to delineate the hepatic vasculature, which was administered intravenously using an automated injector system (CT 9000; Liebel-Flarsheim, Cincinnati, OH) at a rate of 2.0 ml/s. Automated bolus tracking with bolus detection on the level of the ascending aorta assured accurate timing of the arterial phase. For display of the portal and hepatic venous anatomy, third and fourth CT image sets were acquired at 10 and 40 s after the arterial imaging [23].

Four steps are required for transferring the CT DICOM file into 3D digital liver using Hisense CAS: [1] upload the primary CT DICOM data into the Hisense CAS; [2] auto or semi-automatically reconstruct the liver structures (liver parenchyma, portal vein, hepatic veins, and tumors) in a 3D context by extraction of neighboring voxels with a similar CT density, and automatically calculate the total liver volume and tumor volume; [3] virtual liver resection using the software (automatically calculating the remnant liver volume); and [4] assessment of the optimal surgical procedures based on the virtual hepatectomy. The surgical team could communicate and discuss the surgical liver anatomy with radiologists or pediatricians based on 3D reconstruction, such as the tumor locations, the appearance of the vessel branches, or approach of liver resection. Various virtual surgical strategies could be explored in the Hisense CAS. Finally, the surgical team could develop the optimal plan of operation [7].

http://dx.doi.org/10.5772/intechopen.73855

5. Dong's digital liver classification

With the development of medical imaging, 3D reconstruction technology, the innovation of liver surgery and the proposal of precision hepatectomy, the intrahepatic vascular anatomy of the liver and liver segmentectomy based on that vascular anatomy have become well developed. With the analysis of 3D digital liver, we proposed a new type of liver classification system: Dong's digital liver classification system. Professor Dong Qian of the Affiliated Hospital of Qingdao University analyzed the anatomy of thousands of digital human livers from newborns to the elderly to build a new system of liver classification based on intrahepatic vascular anatomy [24].

1260 cases of normal human liver were rendered into 3D digital livers using their DICOM files. Based on the anatomical variation of the portal branches supplying liver segments, we built our Dong's digital liver classification system.

We divided the digital liver into four groups based on the type of segmentation and the variations in portal vein anatomy. Type A livers are similar to Couinaud or Cho's segmentation, containing eight segments (**Figure 5**). Type B livers have nine segments because there are three subdivisions of right-anterior portal vein (**Figure 6**). The defining characteristic of Type C is the variation in the right-posterior portal vein, which is arcuate-shaped (**Figure 7**). Type C-a livers have arcuate-shaped right-posterior portal veins and right-anterior portal veins like those in Type A livers. Type C-b livers have arcuate-shaped right-posterior portal veins and right-anterior portal veins like those in Type B livers. Type D livers have anomalous portal vein variations, which require three-dimensional simulation and individualized liver resection plan (**Figure 8**).

Type A: Similar to Couinaud [25] or Cho's segmentation [26], containing eight segments (**Figure 5**).

Segment I (3–6 P1 branches): Caudate lobe. There are 3–6 small branches (P1) originating from the back of right and left portal vein, surrounded by 5–8 tiny short hepatic veins.

Segments II and III: The left portal vein divides into the third-grade portal vein (P2 and P3) and perfuses the upper and lower outer sides of the left liver, which contains segments II and III.

Segment IV: Portal veins divided from the left portal vein perfuse the inner part of the left liver.

Segments V and VIII: The right portal vein divides into the right anterior and posterior branches, and then the anterior trunk further divides into several branches. (**Figure 5**).

Segments VI and VII: The right posterior portal vein further divides into right anterior (P6) and posterior branches (P7). The anterior branches perfuse segment VI, the lower outer area of the right liver.

Type B: Nine segments due to three subdivisions of right-anterior portal vein (**Figure 6**).

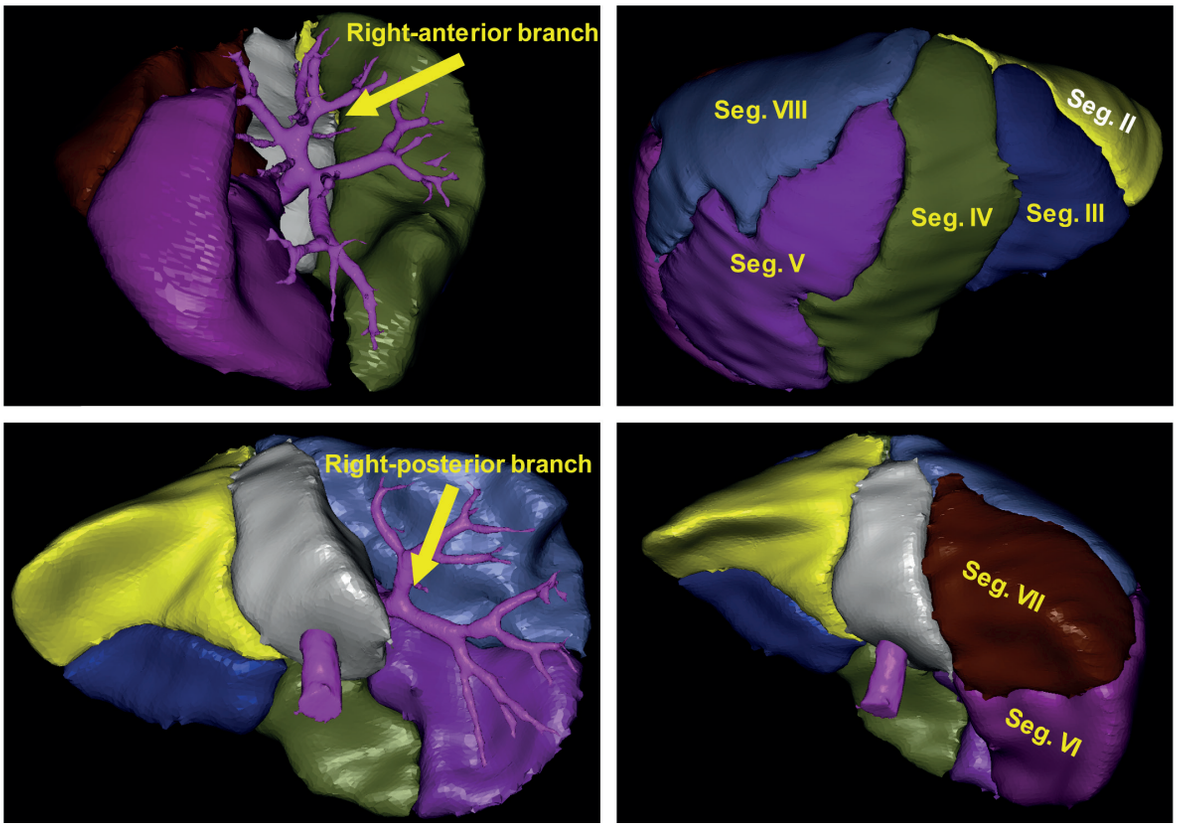

Figure 5. Right-anterior and right-posterior part of liver anatomy indicating Type A segmentation of Dong's digital liver classification system, similar to Couinaud or Cho's segmentation.

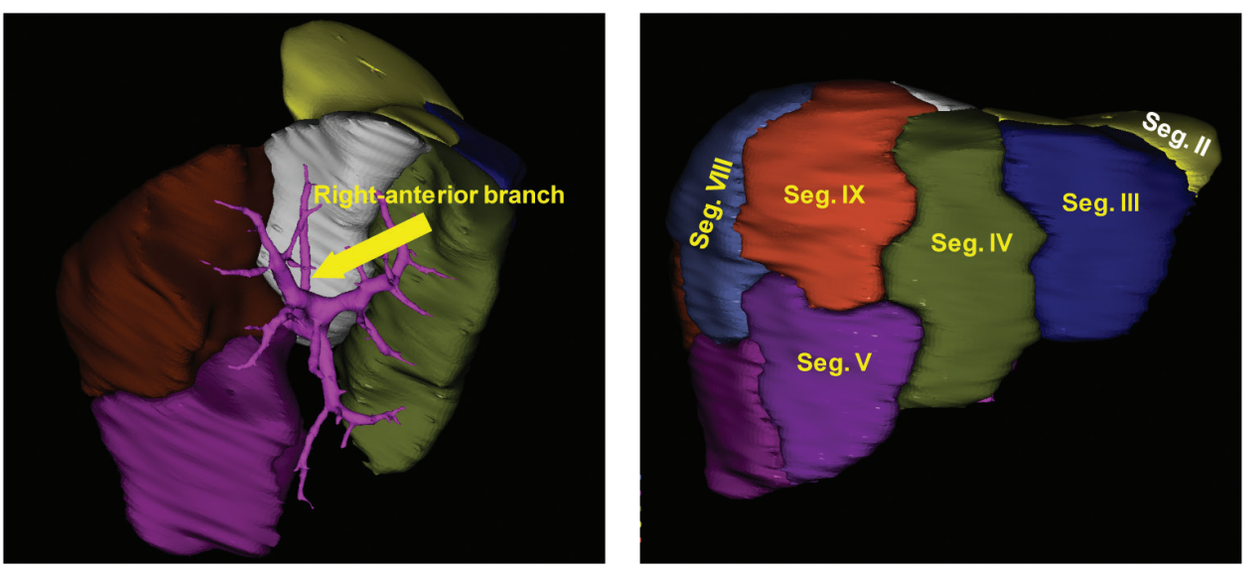

Figure 6. Right-anterior part of liver anatomy indicating Type B segmentation of Dong's digital liver classification system.

http://dx.doi.org/10.5772/intechopen.73855

Type C: The right posterior portal vein does not divide into main branches as in Type A or B livers, whose portal veins separate into 5–11 branches from an arcuate trunk. During precise hepatectomy, it is difficult to resect only segments VI or VII as in Type A and Type B. The prevalence of Type C livers is not high, but it makes a considerable difference in precise surgery. Cases in which the right posterior portal vein is arcuate type and the right anterior portal vein separates into only P8 and P5 are defined as Type C-a (**Figure 7**). When the right posterior portal vein is arcuate type and the right anterior portal vein separate to P5, P8, and P9, we define it as Type C-b.

Type D: This is a catchall category, appearing in about 12.43% of all livers. It includes all variations that cannot be classified into any of the previous three types (**Figure 8**).

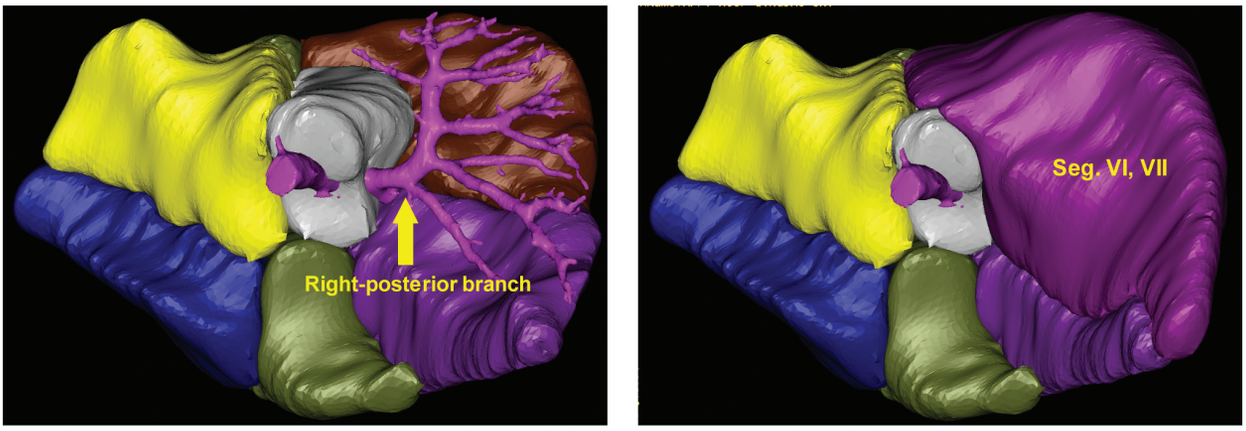

Figure 7. Type C livers have arcuate-shaped right-posterior portal veins.

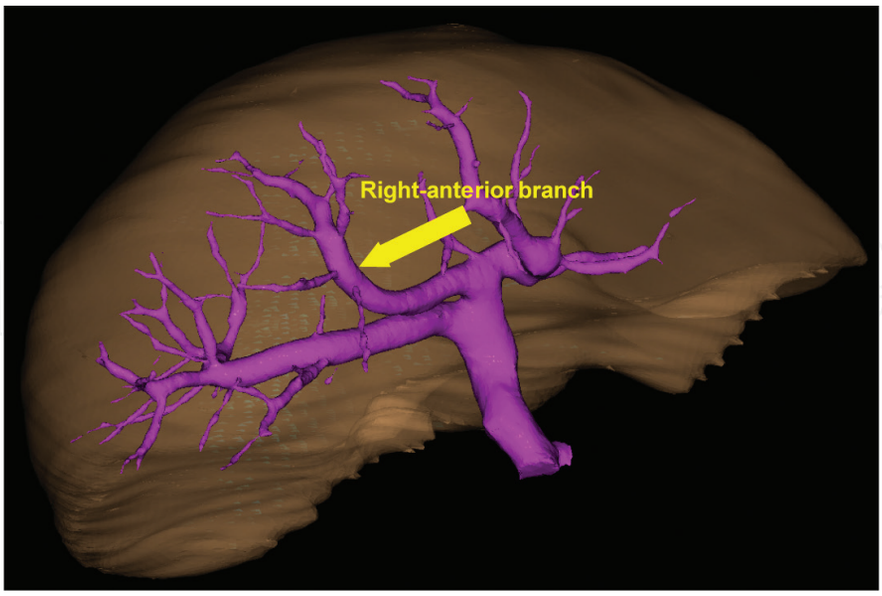

Figure 8. Rare variation of portal vein which is classified into Type D segmentation.

6. Measurement of liver volume from neonates to the elderly

Total liver volume, the basic unit of liver function, is an important factor to evaluate the resectability of liver cancer. There have been many studies of the total liver volume and necessary remnant liver volume in adult patients but only a few reports regarding liver volume in children. Because measured total liver volume has been proposed as the golden standard of liver volume for preoperative surgical plan, we tried to summarize the average total liver volume of Chinese patients of different ages, from neonates to the elderly.

Age	N	Liver volume (cm^3)
<1 Month	28	140.0339 ± 50.0707
1–3 Months	26	191.1462 ± 38.9132
4–6 Months	31	261.5065 ± 70.9437
7–9 Months	22	273.1917 ± 50.0732
10–12 Months	33	305.4692 ± 36.3323
1–2 Years	56	374.3617 ± 65.8447
2–3 Years	66	440.8111 ± 71.4779
3–4 Years	58	500.0037 ± 103.2837
4–5 Years	49	549.4533 ± 84.6325
5–6 Years	33	639.4677 ± 126.7067
6–7 Years	44	722.0357 ± 140.8796
7–8 Years	44	824.6372 ± 137.9766
8–9 Years	32	844.4633 ± 93.6353
9–10 Years	37	935.8571 ± 189.1018
10–11 Years	29	985.0464 ± 121.0802
11–12 Years	27	1048.9250 ± 167.5279
12–13 Years	29	1118.4593 ± 155.2817
13–14 Years	22	1125.0250 ± 147.9899
14–18 Years	30	1323.8862 ± 226.3454
18–30 Years	42	1361.8682 ± 205.3783
30–40 Years	74	1381.1037 ± 300.3834
40–50 Years	139	1423.7647 ± 216.9305
50–60 Years	197	1343.2768 ± 246.6878
60–70 Years	181	1284.4183 ± 190.7129
70–80 Years	106	1263.1282 ± 170.2464
80–100 Years	21	1089.3429 ± 199.0259
Total	1456	

Table 1. Standard liver volume range (X ± S, cm^3).

Upper abdominal CT films from 1456 children (enhanced CT 837, plain CT 619) aged 1 day to 100 years were selected. None had any history of liver disease, and CT had been performed for other clinical purposes. The patients were divided into 26 groups by age (**Table 1**).

7. Human Digital Liver Database

The Human Digital Liver Database (HDLD) was established by the Affiliated Hospital of Qingdao University and Hisense Company, aiming to collect digital liver from neonates, children, adults, and the elderly, from normal livers, livers with cancer, and simulated livers resected using Hisense CAS. The link of the HDLD is http://www.hdldb.net, which now is only available in Chinese (the English version is being translated now). The HDLD will show the digital liver in image and video form. All visitors could study the updated clinical cases at any angle of reconstructed 3D digital liver, including the vascular system, anatomical differences in the liver, and the correlation between vascular and liver tumors. The HDLD will also provide the intra-operation video comparing to the preoperative surgical plan, to help doctors and medical students better understand the anatomy and surgical procedure of pediatric liver resection, especially for patients with giant liver tumors (**Figure 9**).

7.1. Normal children and adult digital liver database

Vascular anatomical variation and total liver volume are two of the more important factors that surgeons consider when making surgical plans. We have collected thousands of CT scan data from across the nation. We would like to establish a digital liver database showing the reconstructed digital liver and separate these digital livers into different groups according to the anatomical variations in liver vasculature and liver volume (**Figure 9**). The Dong's Digital Liver Classification was established based on our collection of digital livers. We believe that a normal digital liver database may serve as an important reference for surgeons all around world.

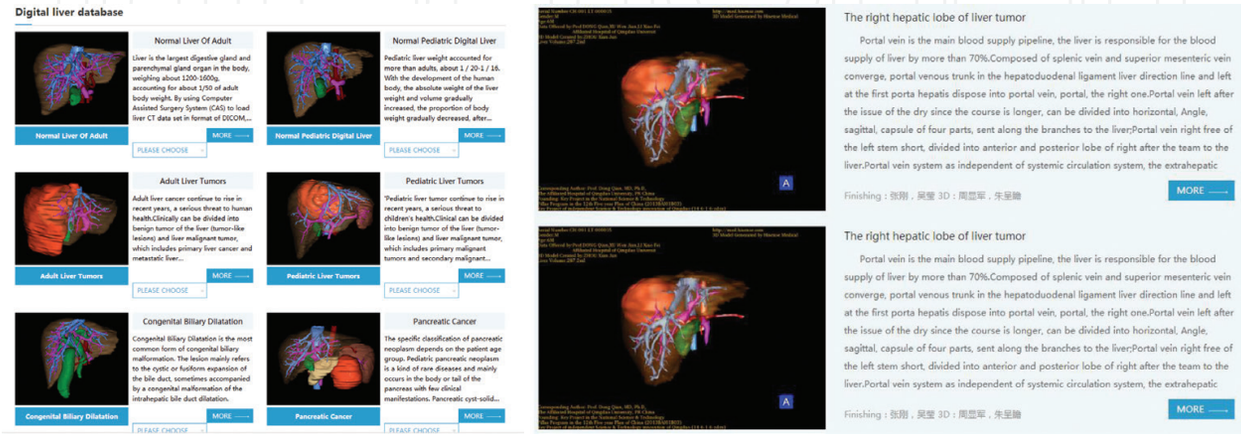

Figure 9. The Human Digital Liver Database.

7.2. Liver tumor database and simulated liver surgery

The liver tumor database shows the reconstructed digital liver image and simulated liver resection according to the surgeon's preoperative plan, and the intraoperative video of clinical cases, aiming to share the experience gained by staff at our center freely around the world. With the help of Hisense CAS, the successful surgical resection of liver tumors in pediatric patients has improved in our center. With the 3D simulation, we have found that we can clearly understand the anatomical variation in intrahepatic vasculature, the correlation of vasculature with liver tumors, and calculate the remnant liver volume of the simulated liver easily. In the database, we would like to show some difficult cases, such as those with very large liver tumors and those with vascular variation.

8. Clinical application of Hisense CAS for diagnosis and surgical plans in children with large liver tumors

An 11-month-old male infant was referred with abdominal distension and loss of appetite for the past 2 months [27]. Upon examination, a firm, non-tender mass with a smooth surface was evident arising from the right lobe of the liver, which filled the abdominal cavity. Serum ALT, AST, GGT, ALP, and Alb were normal. Both serum α-fetoprotein (AFP) and carcinoembryonic antigen (CEA) levels were within normal ranges. Ultrasound (US) revealed a well-defined, multicystic mass involving the liver. Enhanced CT images similarly showed a giant cystic mass with minimally enhanced septation and peripheral solid components (**Figure 10**).

The DICOM data obtained from the CT images were uploaded to 3D simulation software, the Hisense Computer Assisted Surgery System (Hisense, China) to simulate the liver. The relationship between HMH and the intrahepatic vasculature was revealed in a 3D context (**Figure 11**). The right hepatic vein (RHV), the middle hepatic vein (MHV), and the left hepatic vein (LHV) were confluent with a common trunk. The hepatic veins (HVs), the portal veins (PVs), and the inferior vena cava (IVC) were displaced, with no obvious infiltration or encasement. The volume of both the functional liver and the HMH was automatically calculated. The positional relationship between the vessels and HMH could be confirmed from any angle instantaneously in the computer. Various virtual hepatectomies were performed to predict the risk and the difficulty of the actual hepatectomy. Finally, an optimal surgical

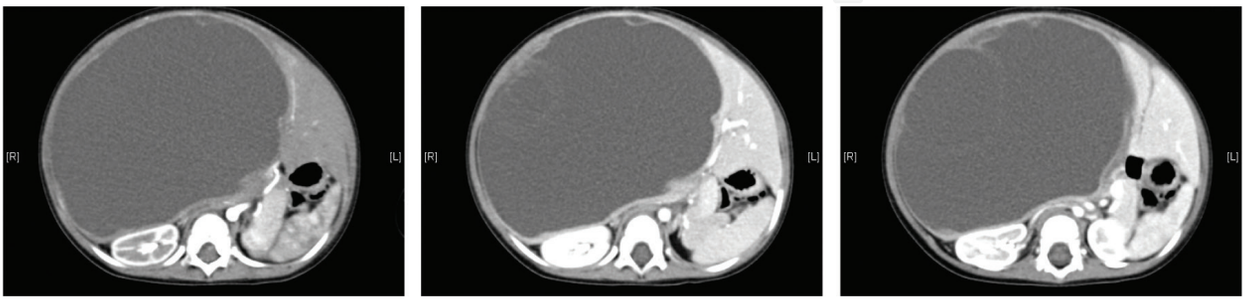

Figure 10. Preoperative enhanced CT scan.

plan was developed using 3D simulation software to safeguard RHV. The enucleation of HMH for the case was performed after adequate preoperative preparation.

After laparotomy, the fluid was aspirated using a 20 G needle from the cystic components of HMH to reduce its volume, thereby facilitating surgical resection. The resection line at the rim of HMH, which was indicated by virtual hepatectomy was made using the electrotome. The hepatic portal occlusion was used to reduce the risk of bleeding. The hepatic parenchyma was dissected using the CUSA system. The intrahepatic vessels were dissected to be safeguarded or else ligated and divided, a matter that had been assessed by the virtual hepatectomy. After 20 min, the HMH was removed with surrounding rim of normal liver tissue. The right hepatic vein was successfully safeguarded. The remnant liver volume was about 210 ml, which approximately equaled the automatically calculated remnant liver volume (230.1 ml). There was no anatomical discrepancy between the operation and the 3D simulation. The convalescence was uneventful. Histopathology confirmed the diagnosis of mesenchymal hamartoma (**Figure 12**).

In summary, three-dimensional (3D) imaging could significantly improve the resection rate of pediatric tumors and increase the safety of the surgery. Dong's digital liver classification system and human digital liver classification system will be useful for surgeons all around the world.

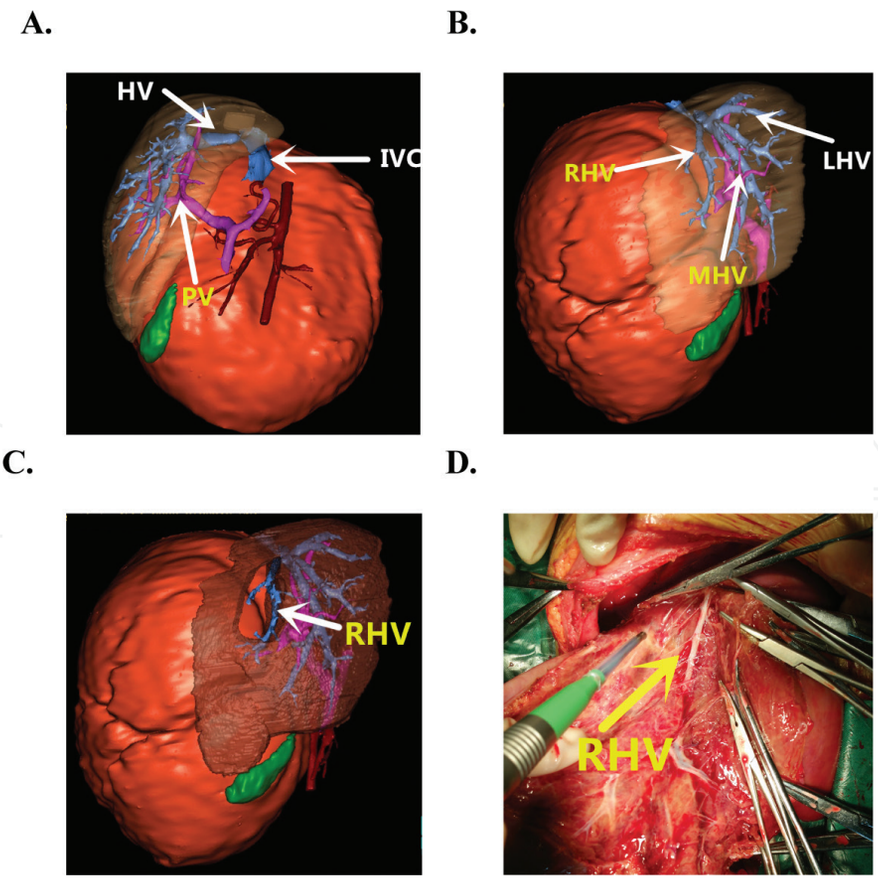

Figure 11. Comparison of 3D simulation and intraoperative liver anatomy.

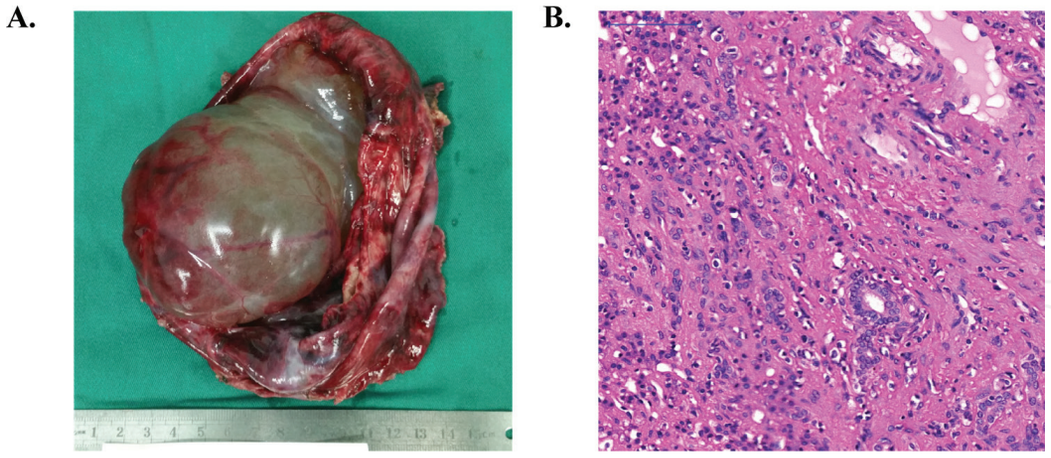

Figure 12. Resected HMH tumor and pathology.

Author details

Chengzhan Zhu[1,4], Bingzi Dong[2] and Qian Dong[3,4]*

*Address all correspondence to: 13608968352@163.com

1 Department of Hepatobiliary and Pancreatic Surgery, The Affiliated Hospital of Qingdao University, Qingdao, China

2 Department of Endocrinology and Metabolism, The Affiliated Hospital of Qingdao University, Qingdao, China

3 Pediatric Surgery Department, The Affiliated Hospital of Qingdao University, Qingdao, China

4 Shandong Key Laboratory of Digital Medicine and Computer Assisted Surgery, The Affiliated Hospital of Qingdao University, Qingdao, China

References

[1] Stocker JT. Hepatic tumors in children. Clinics in Liver Disease. 2001;**5**(1):259-281 viii-ix

[2] LaBerge JM. Liver tumors. In: O'Neill JA Jr, Grosfeld JL, Fonkalsrud EW, et al., editors. Principles of Pediatric Surgery. 2nd ed. St Louis: Mosby; 2003

[3] Yikilmaz A, George M, Lee EY. Pediatric hepatobiliary neoplasms: An overview and update. Radiologic Clinics of North America. 2017;**55**(4):741-766

[4] De Ugarte DA, Atkinson J. Liver tumors. In: Grosfeld JL, O'Neill JA Jr, Fonkalsrud AG, Coran AG, editors. Pediatric Surgery. 6th ed. Philadelphia: Mosby-Elsevier; 2006. pp. 502-505

[5] Aronson DC, Meyers RL. Malignant tumors of the liver in children. Seminars in Pediatric Surgery. 2016;**25**(5):265-275

[6] Roebuck DJ. Assessment of malignant liver tumors in children. Cancer Imaging. 2009; **9 Spec No A**:S98-S103

[7] Zhang G, Zhou XJ, Zhu CZ, Dong Q, Su L. Usefulness of three-dimensional(3D) simulation software in hepatectomy for pediatric hepatoblastoma. Surgical Oncology. 2016;**25**(3):236-243

[8] Czauderna P, Haeberle B, Hiyama E, Rangaswami A, Krailo M, Maibach R, et al. Novel global rare tumor database yields new prognostic factors in hepatoblastoma and becomes a research model. European Journal of Cancer. 2016;**52**:92-101

[9] Brown J, Perilongo G, Shafford E, Keeling J, Pritchard J, Brock P, et al. Pretreatment prognostic factors for children with hepatoblastoma-- results from the International Society of Paediatric Oncology (SIOP) study SIOPEL 1. European Journal of Cancer. 2000;**36**(11):1418-1425

[10] Czauderna P, Otte JB, Aronson DC, Gauthier F, Mackinlay G, Roebuck D, et al. Guidelines for surgical treatment of hepatoblastoma in the modern era--recommendations from the Childhood Liver Tumour Strategy Group of the International Society of Paediatric Oncology (SIOPEL). European Journal of Cancer. 2005;**41**(7):1031-1036

[11] Dong Q, Chen J. CT scan of pediatric liver tumors. In: Subburaj K, editor. CT Scanning Techniques and Applications. Intech; 2011

[12] Darbari A, Sabin KM, Shapiro CN, Schwarz KB. Epidemiology of primary hepatic malignancies in U.S. children. Hepatology. 2003;**38**(3):560-566

[13] Czauderna P, Mackinlay G, Perilongo G, Brown J, Shafford E, Aronson D, et al. Hepatocellular carcinoma in children: Results of the first prospective study of the International Society of Pediatric Oncology group. Journal of Clinical Oncology. 2002;**20**(12): 2798-2804

[14] Agarwala S. Primary malignant liver tumors in children. The Indian Journal of Pediatrics. 2012;**79**(6):793-800

[15] Su L, Dong Q, Zhang H, Zhou X, Chen Y, Hao X, et al. Clinical application of a three-dimensional imaging technique in infants and young children with complex liver tumors. Pediatric Surgery International. 2016;**32**(4):387-395

[16] Shoup M, Gonen M, D'Angelica M, Jarnagin WR, DeMatteo RP, Schwartz LH, et al. Volumetric analysis predicts hepatic dysfunction in patients undergoing major liver resection. Journal of Gastrointestinal Surgery. 2003;**7**(3):325-330

[17] Austin MT, Leys CM, Feurer ID, Lovvorn HN 3rd, O'Neill JA Jr, Pinson CW, et al. Liver transplantation for childhood hepatic malignancy: A review of the United Network for Organ Sharing (UNOS) database. Journal of Pediatric Surgery. 2006;**41**(1):182-186

[18] Plant AS, Busuttil RW, Rana A, Nelson SD, Auerbach M, Federman NC. A single-institution retrospective cases series of childhood undifferentiated embryonal liver sarcoma (UELS): Success of combined therapy and the use of orthotopic liver transplant. Journal of Pediatric Hematology/Oncology. 2013;**35**(6):451-455

[19] Cao Q, Ye Z, Chen S, Liu N, Li S, Liu F. Undifferentiated embryonal sarcoma of liver: A multi-institutional experience with 9 cases. International Journal of Clinical and Experimental Pathology. 2014;**7**(12):8647-8656

[20] Hashimoto D, Dohi T, Tsuzuki M, Horiuchi T, Ohta Y, Chinzei K, et al. Development of a computer-aided surgery system: Three-dimensional graphic reconstruction for treatment of liver cancer. Surgery. 1991;**109**(5):589-596

[21] Lamade W, Glombitza G, Fischer L, Chiu P, Cardenas CE Sr, Thorn M, et al. The impact of 3-dimensional reconstructions on operation planning in liver surgery. Archives of Surgery. 2000;**135**(11):1256-1261

[22] Souzaki R, Ieiri S, Uemura M, Ohuchida K, Tomikawa M, Kinoshita Y, et al. An augmented reality navigation system for pediatric oncologic surgery based on preoperative CT and MRI images. Journal of Pediatric Surgery. 2013;**48**(12):2479-2483

[23] Fuchs J, Warmann SW, Szavay P, Kirschner HJ, Schafer JF, Hennemuth A, et al. Three-dimensional visualization and virtual simulation of resections in pediatric solid tumors. Journal of Pediatric Surgery. 2005;**40**(2):364-370

[24] Zhou X, Dong Q, Zhu C, Chen X, Wei B, Duan Y, et al. The role and significance of digital reconstruction technique in liver segments based on portal vein structure. Chinese Journal of Surgery. 2018;**56**(1):61-67

[25] Couinaud C. The anatomy of the liver. Annali Italiani di Chirurgia. 1992;**63**(6):693-697

[26] Cho A, Okazumi S, Miyazawa Y, Makino H, Miura F, Ohira G, et al. Proposal for a reclassification of liver based anatomy on portal ramifications. American Journal of Surgery. 2005;**189**(2):195-199

[27] Zhao J, Zhou XJ, Zhu CZ, Wu Y, Wei B, Zhang G, et al. 3D simulation assisted resection of giant hepatic mesenchymal hamartoma in children. Computer Assisted Surgery (Abingdon). 2017;**22**(1):54-59